

# Enhanced Transcranial Ultrasonic Imaging utilizing Dual Frequency Transducers

Amanatiadis Stamatios<sup>1,2</sup>, Apostolidis Georgios<sup>1,2</sup>, Bekiari Chrysanthi<sup>3</sup>, Nikolaos Kantartzis<sup>1</sup>

<sup>1</sup> Aristotle University of Thessaloniki, Dept. of Electrical and Computer Eng., Thessaloniki, Greece, kant@auth.gr

<sup>2</sup> Ormylia Foundation, Art Diagnosis Center, Ormylia, Greece, samanati@auth.gr

<sup>3</sup> Aristotle University of Thessaloniki, Faculty of Veterinary Medicine, Thessaloniki, Greece, chmpekia@vet.auth.gr

**Abstract**—In the present work the development of a dual frequency ultrasonic imaging method is proposed to assist the transcranial acoustic wave propagation for medical applications. This method depends on the significantly altered acoustic properties of the skull, compared to the soft brain tissues, mainly on the increased absorption coefficient. The latter leads in a differentiated acoustic wave propagation at separate frequencies and the fusion of the acquired data provide an enhanced perception of the inner, to the skull, regions. The theoretical analysis is performed based on realistic human skull and brain tissue properties, while it is validated via an accurate numerical model, both in A-scan and B-scan modes.

## I. INTRODUCTION

Brain imaging is one of the most crucial areas in medical applications due to its importance in the life and functionality of a human. Several defects and malfunctions brain's inner structure can be detected through various non-invasive imaging techniques [1]–[3] that are achieving either through taking into advantage the different properties of the brain tissues or through the brain functionality and activity. The former includes the popular Magnetic Resonance Imaging (MRI) and the Computed Tomography (CT) scanning, while the latter is utilized from functional MRI (fMRI), Positron Emission Tomography (PET), Electroencephalography (EEG), Magnetoencephalography (MEG) etc. Although, each method has specific advantages, such as the high resolution of MRI, CT, fMRI and PET and the very fast temporal response of EEG and MEG, there are some basic disadvantages, including either an expensive method or a very low resolution of the brain's inner structure.

Until this point, there is not any reference on ultrasonic imaging, one of the most popular non-invasive techniques. Ultrasonic imaging is based on the propagation of the acoustic waves and the tomographic reconstruction through the multiple reflections of the inner details. It is a very safe, cheap and accurate non-invasive technique that has an application on several medical examinations that include abdominal, heart and other soft body parts. The latter observation is the main reason that despite its attractive features, ultrasonography has a limited application on human brain due to the physically hard structured skull. Specifically, the acoustic properties of a material depend on its elasticity and density; consequently the bones exhibit significantly different features compared to other soft tissues and the propagation of an acoustic wave beyond

a bone, such as the brain, is severely degraded because of the skull's scattering properties. Nevertheless, there are some approaches that utilize ultrasonic waves either for therapeutic [4], [5] or imaging purposes. Concerning the latter, where the current work focuses, there are studies that conventional ultrasound techniques are able to detect regions of interest through simple image processing algorithms [6], [7]. Moreover, the application of dual arrays of transducers at opposite sides of the head is proposed to create a fused tomographic image [8]–[10], while image enhancement is predicted through the phase correction of the received signal [11] and multiplanar transcranial images [12].

The present work acts additive to the previous proposed techniques for the further enhancement of the tomographic imaging of brain. Our method depends on the diversity, in terms of the acoustic properties, of the skull bone compared to the soft inner brain tissues taking into advantage the high attenuation inside the skull. To this end, a dual frequency [13]–[16] operation is performed and the received signals are fused to neglect the influence of the bone and reveal the inner details. Initially, a simplified but realistic one-dimensional model is designed and the reduction of the skull effect is studied analytically. Then, the theoretical approach is validated via an accurate numerical algorithm that utilizes the efficient k-space method [17], [18]. Finally, tomographic B-scans are acquired through acoustic propagation simulations using phased-array transducers of coupled frequency elements.

## II. THEORETICAL ASPECTS

Ultrasonography is an excellent modality for the acquisition of tomographic images and the sub-surface characterization of complex structures. This fact arises from the ability of acoustic waves to penetrate easily the majority of the materials, unlike the electromagnetic ones. Moreover, very fine imaging resolution is achieved at low cost designating the ultrasounds an exceptional tool for medical applications. However, its operation is limited in soft regions, such as abdomen, heart and lungs, due to the signal degradation that hard parts, like bones and skull, import. Specifically, the acoustic properties of bones are diverging from the soft tissues, as depicted in Table I, introducing high scattering and attenuation at an incident acoustic wave.

TABLE I  
ACOUSTIC PROPERTIES OF COUPLING MATERIAL AND HUMAN HEAD TISSUES AND SKULL AT 1 MHz [19]–[21].

Material	Hydrogel	Bone	CSF	Gray matter	White matter
Acoustic velocity (m/s) $c$	1540	2850	1500	1550	1600
Density (kg/m <sup>3</sup> ) $\rho$	1000	1900	1000	1050	1030
Attenuation coefficient (dB/cm) $\alpha$	0.002	11	0.8	0.8	0.8
Absorption power $y$	1.5	0.6	1.5	1.1	1.1

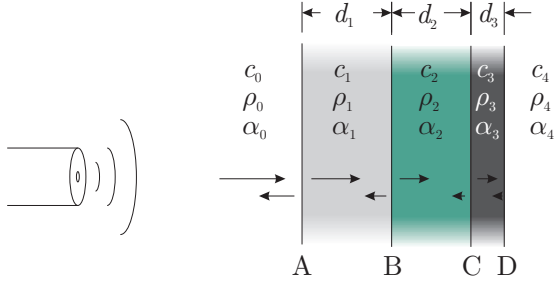


Fig. 1. Analysis setup comprised of hydrogel, bone of  $d_1 = 8$  mm thickness,  $d_2 = 7$  mm thick cerebrospinal fluid layer, gray matter of  $d_3 = 4$  mm and white matter (subscripts from 0 – 4 respectively).

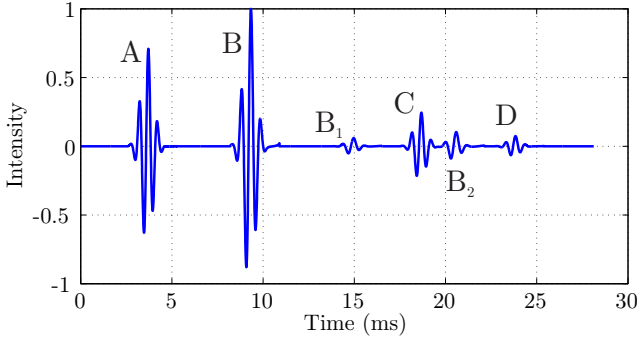


Fig. 2. An A-scan of the setup under investigation after time gain compensation.

Concerning the ultrasonic imaging of a human head, the initial problem is the extremely weak echoes from the deeper layers of the head due to the abovementioned characteristics of the skull. The energy of the acoustic waves, generated by the ultrasonic transducer, is attenuating exponentially as the wave propagates inside the tissues

$$p = p_0 e^{-\alpha f^y d}, \quad (1)$$

where  $p$  and  $p_0$  are the resulting and the initial acoustic pressure, respectively,  $f$  is the frequency,  $d$  the propagating distance and  $\alpha$  is the attenuation coefficient. For this reason, a time gain compensation algorithm is utilized to reverse the effect of attenuation.

However, one other main problem appears that is the echoes due to the multiple reflections. Consider the setup of Fig. 1, where multiple reflections occur rapidly on interface B due to the high acoustic velocity of skull. Specifically, an acquired A-scan, namely a point measurement, from this setup, after

the time gain compensation, is illustrated in Fig. 2. Here the echoes  $B_1$  and  $B_2$ , that correspond to multiple reflection at the backside of the skull, are preceding to the ones at interfaces C and D that physically represent the limits of cerebrospinal fluid (CSF) and gray matter. Consequently, the final image reconstruction presents artefacts and advanced techniques need to be applied in order to eliminate them.

In our work, the disadvantage of the skull's high attenuation is turned into an advantage through the consideration of the propagation losses dependence on the frequency, concerning (1). In particular, the echoes that correspond to the multiple reflections inside the skull suffer stronger losses with the increment of frequency. Consequently, these echoes can be distinguished easily using two distinct stimulating frequencies and we propose a dual frequency ultrasonic module to enhance the brain imaging.

The proposed method is studied theoretically through the consideration of the input acoustic signals of Fig. 3a and the investigation of their propagation via the several layers of Fig. 1. The reflection  $R$  and transmission  $T$  energy coefficients at each interface are calculated

$$R = \left( \frac{Z_m - Z_n}{Z_m + Z_n} \right)^2, \quad (2a)$$

$$T = 1 - R, \quad (2b)$$

where  $Z_i = c_i \rho_i$  is the acoustic impedance of material  $i$  and  $m, n$  correspond to the subscripts of Fig. 1. Moreover, the input signals are Fourier-transformed (Fig. 3b) and

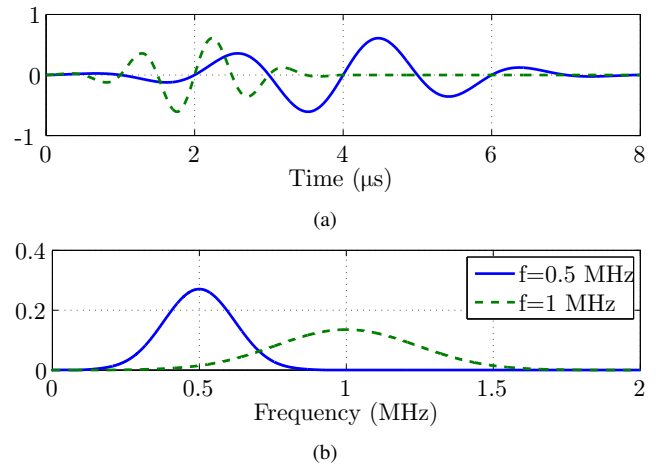


Fig. 3. (a) Excitation signals and (b) their corresponding spectra.

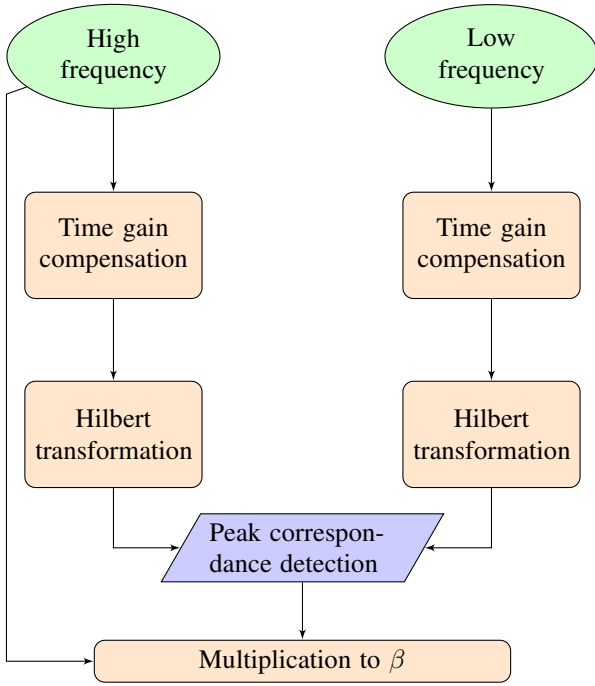


Fig. 4. Flow chart describing the dual frequency module processing.

the propagation attenuation at each frequency is calculated via (1) before the inverse transformation. To this end, the strength of the various echoes is extracted and the A-scan signal is acquired based on the propagation time inside the materials. The A-scan is further processed via the time gain compensation algorithm, while a Hilbert transform is applied to extract the analytic signal [22]. The resulting A-scans from the two different stimulating frequencies are illustrated in Fig. 5, where it is obvious that the echoes due to multiple reflections are significantly lowered at the higher stimulating frequency. However, the echoes are still distinguishable and for this reason the two A-scans are further processed and fused to generate an artefact free signal. Initially, the peaks of the echoes are detected and the ones of the high frequency signal are multiplied to the ratio

$$\beta_j = \frac{A_{f_h j}}{A_{f_l j}}, \quad (3)$$

where  $A_{f_h j}$  and  $A_{f_l j}$  is the magnitude of peak  $j$  of the high and low frequency input signals, respectively. The whole process is summarized in Fig. 4, while the artefact free signal is depicted in Fig. 6, proving the performance of the proposed method. Note that if a phantom echo, e.g.  $B_2$ , coincides to an inner one, e.g. C, the algorithm is still valid since the contribution of the inner echo prevents the amplitude of the high frequency signal to decrease significantly.

### III. NUMERICAL VALIDATION

The validity of the proposed dual frequency ultrasonic module is further investigated via numerical analysis of the equivalent setup in Fig. 1. The simulations are performed

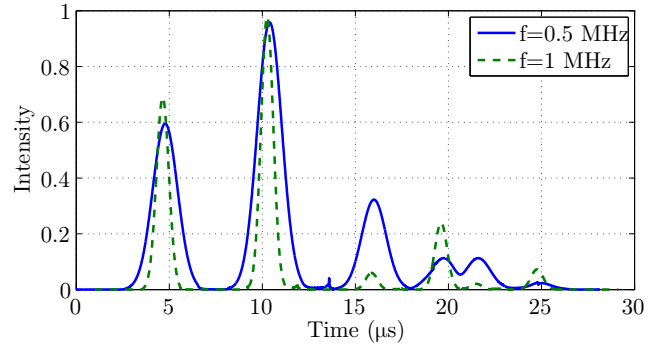


Fig. 5. Hilbert transformed analytically extracted A-scans after time gain compensation processing.

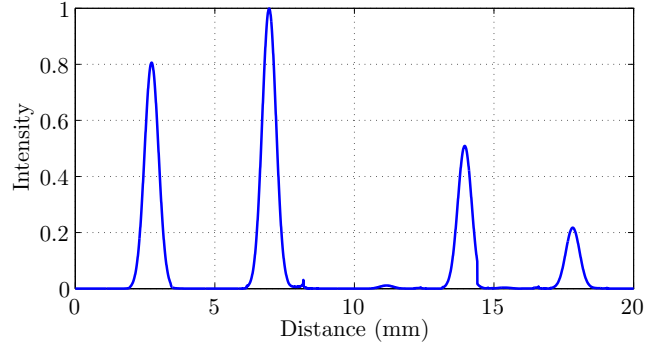


Fig. 6. Enhanced analytically extracted A-scan via fusion of the dual frequency module.

via the accurate k-Wave MATLAB toolbox because of the flexibility and the efficiency of the k-space algorithm [23]. First of all, the one-dimensional problem is solved in order to correspond to the A-scan acquired via the theoretical analysis of the previous section. The computational domain is divided in 140 cells of  $\Delta x = 200 \mu\text{m}$ , the time-step is selected  $\Delta t = 21 \text{ ns}$  and the open boundaries are terminated via a 10-cell thick Perfectly Matched Layer (PML). The dual frequency module is utilized on the simulations and the A-scans are demonstrated in Fig. 7 after the time gain compensation and Hilbert transform processing. Note, that a noise factors are,

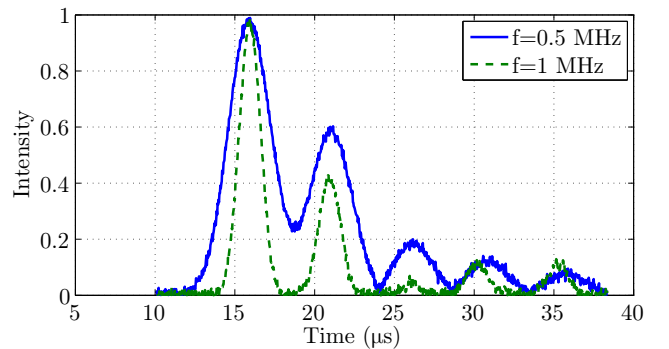


Fig. 7. Hilbert transformed numerically extracted A-scans after time gain compensation processing.

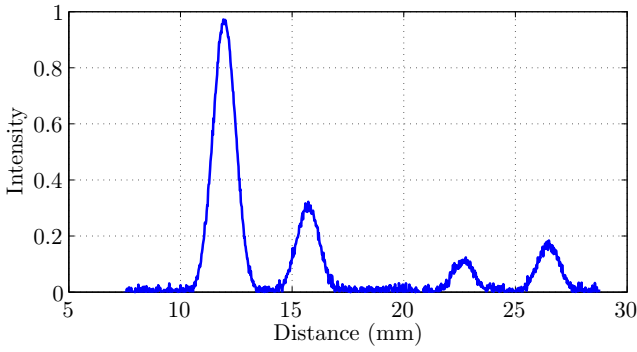


Fig. 8. Enhanced numerically extracted A-scan via fusion of the dual frequency module.

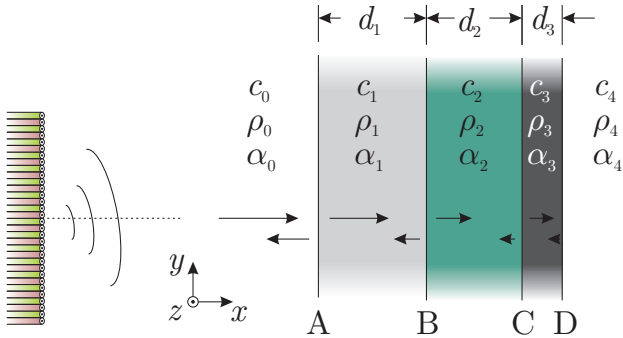


Fig. 9. Equivalent to Fig. 1 volumetric setup stimulated via a dual frequency phased array.

also, added at the sensor in order to approximate the real-life scenario. Specifically, the noise is considered as a normal distribution of zero mean value and a typical 1% of the signal amplitude standard deviation. It is obvious that the artefacts due to the multiple reflections are appearing near  $25 \mu s$ . However, the application of the fusion process of Fig. 4 is able to clear the A-scan as depicted in Fig. 8 verifying our method's performance.

Moreover, a more realistic three-dimensional counterpart to the previous study is numerically investigated in order to extract B-scans, namely the combination of A-scans to acquire tomographic images. The setup is described in Fig. 9 and the dual frequency module is now implemented on a phased array transducer. Particularly, the high and low frequency transducers interchange, thus a single probe is required. The simulation is performed via the three-dimensional k-Wave MATLAB toolbox and the computational domain is discretized in  $130 \times 70 \times 70$  cells of  $\Delta x = \Delta y = \Delta z$ , while time-step is set to 40 ns and the open boundaries are truncated via a 10-cell thick PML. The phased array sweeps the area from  $-16^\circ$  to  $16^\circ$  with respect to  $x$ -axis and each scan line is processed according to the described steps, namely the time gain compensation and the Hilbert transformation. The B-scan images in Fig. 10 for the two frequencies separately reveal that the artefacts due to the multiple reflections are still present, despite the advanced processing of the phased array. This artefacts, though, are neglected at the fused image proving

the proposed method's additive enhancement to conventional ultrasonic imaging techniques.

#### IV. CONCLUSION

In this paper, the enhancement of an ultrasonic tomographic image for transcranial medical application via a dual frequency module is proposed. The theoretical study indicated that the artefacts due to the multiple reflections at the backside of the highly scattering and attenuating skull are diminished utilizing the proposed technique. Consequently, the imaging of inner structure is clearer, revealing possible tissue anomalies. Moreover, the method's performance has been further verified by means of a numerical investigation for both single A-scans and B-scan tomographic images.

#### ACKNOWLEDGMENT



Operational Programme  
Human Resources Development,  
Education and Lifelong Learning  
Co-financed by Greece and the European Union



This research is co-financed by Greece and the European Union (European Social Fund- ESF) through the Operational Program "Human Resources Development, Education and Lifelong Learning 2014-2020" in the context of the project "Design of a non-invasive system for brain defect detection using ultrasonography" (MIS 5005360).

#### REFERENCES

- [1] M. Wintermark, M. Sesay, E. Barbier, K. Borbély, W. P. Dillon, J. D. Eastwood, T. C. Glenn, C. B. Grandin, S. Pedraza, J.-F. Soustiel *et al.*, "Comparative overview of brain perfusion imaging techniques," *Stroke*, vol. 36, no. 9, pp. e83–e99, 2005.
- [2] W. H. Oldendorf, "The quest for an image of brain a brief historical and technical review of brain imaging techniques," *Neurology*, vol. 28, no. 6, pp. 517–517, 1978.
- [3] M. E. Shenton, H. Hamoda, J. Schneiderman, S. Bouix, O. Pasternak, Y. Rathi, M.-A. Vu, M. P. Purohit, K. Helmer, I. Koerte *et al.*, "A review of magnetic resonance imaging and diffusion tensor imaging findings in mild traumatic brain injury," *Brain imaging and behavior*, vol. 6, no. 2, pp. 137–192, 2012.
- [4] T. Hölscher, W. G. Wilkening, S. Molkenstruck, H. Voit, and C. Koch, "Transcranial sound field characterization," *Ultrasound in medicine & biology*, vol. 34, no. 6, pp. 973–980, 2008.
- [5] G. Clement and K. Hynynen, "A non-invasive method for focusing ultrasound through the human skull," *Physics in Medicine & Biology*, vol. 47, no. 8, p. 1219, 2002.
- [6] T. Hölscher, W. Wilkening, B. Draganski, S. H. Meves, J. Eyding, H. Voit, U. Bogdahn, H. Przuntek, and T. Postert, "Transcranial ultrasound brain perfusion assessment with a contrast agent-specific imaging mode: results of a two-center trial," *Stroke*, vol. 36, no. 10, pp. 2283–2285, 2005.
- [7] S. Behnke, D. Berg, M. Naumann, and G. Becker, "Differentiation of parkinson's disease and atypical parkinsonian syndromes by transcranial ultrasound," *Journal of Neurology, Neurosurgery & Psychiatry*, vol. 76, no. 3, pp. 423–425, 2005.
- [8] F. Vignon, J.-F. Aubry, M. Tanter, A. Margoum, M. Fink, and J. Lecoqeur, "Dual-arrays brain imaging prototype: Experimental in vitro results," in *Ultrasonics Symposium, 2005 IEEE*, vol. 1. IEEE, 2005, pp. 504–507.
- [9] F. Vignon, J. Aubry, M. Tanter, A. Margoum, and M. Fink, "Adaptive focusing for transcranial ultrasound imaging using dual arrays," *The Journal of the Acoustical Society of America*, vol. 120, no. 5, pp. 2737–2745, 2006.

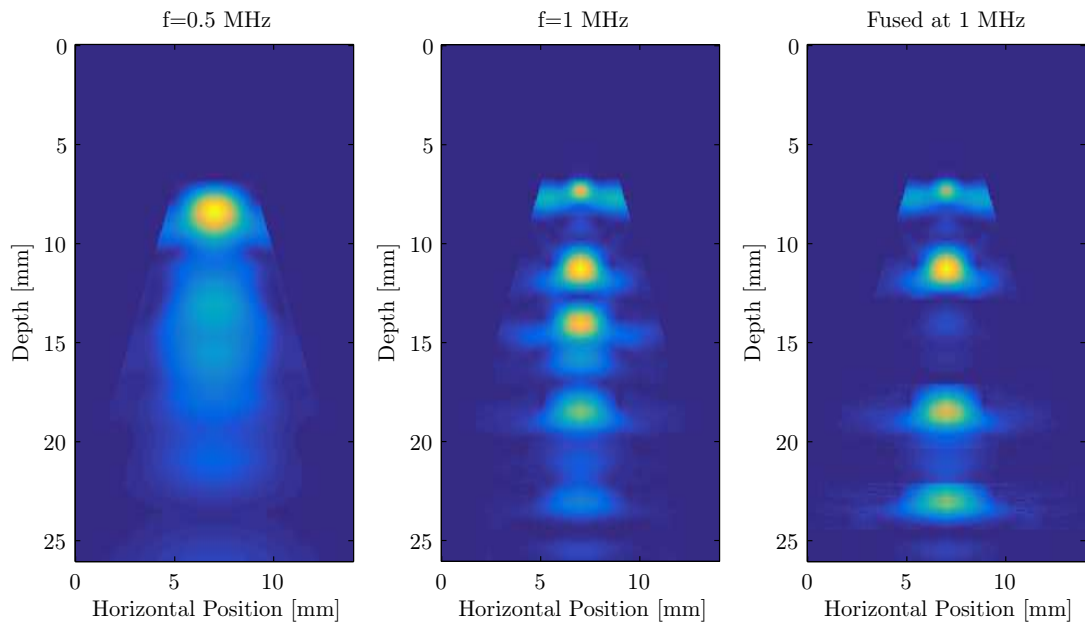


Fig. 10. B-scans of the dual frequency module, separately and as the enhanced fused image.

- [10] B. D. Lindsey, E. D. Light, H. A. Nicoletto, E. R. Bennett, D. T. Laskowitz, and S. W. Smith, "The ultrasound brain helmet: new transducers and volume registration for in vivo simultaneous multi-transducer 3-d transcranial imaging," *IEEE transactions on ultrasonics, ferroelectrics, and frequency control*, vol. 58, no. 6, pp. 1189–1202, 2011.
- [11] T. Wang and Y. Jing, "Transcranial ultrasound imaging with speed of sound-based phase correction: a numerical study," *Physics in Medicine & Biology*, vol. 58, no. 19, p. 6663, 2013.
- [12] R. Kern, F. Perren, S. Kreisel, K. Szabo, M. Hennerici, and S. Meairs, "Multiplanar transcranial ultrasound imaging: standards, landmarks and correlation with magnetic resonance imaging," *Ultrasound in medicine & biology*, vol. 31, no. 3, pp. 311–315, 2005.
- [13] A. H. Barati, M. Mokhtari-Dizaji, H. Mozdarani, Z. Bathaie, and Z. M. Hassan, "Effect of exposure parameters on cavitation induced by low-level dual-frequency ultrasound," *Ultrasonics sonochemistry*, vol. 14, no. 6, pp. 783–789, 2007.
- [14] J. Karjalainen, J. Töyräs, T. Rikonen, J. Jurvelin, and O. Riekkinen, "Dual-frequency ultrasound technique minimizes errors induced by soft tissue in ultrasound bone densitometry," *Acta Radiologica*, vol. 49, no. 9, pp. 1038–1041, 2008.
- [15] R. Gessner, M. Lukacs, M. Lee, E. Cherin, F. S. Foster, and P. A. Dayton, "High-resolution, high-contrast ultrasound imaging using a prototype dual-frequency transducer: in vitro and in vivo studies," *IEEE transactions on ultrasonics, ferroelectrics, and frequency control*, vol. 57, no. 8, pp. 1772–1781, 2010.
- [16] J. Zheng, Q. Li, A. Hu, L. Yang, J. Lu, X. Zhang, and Q. Lin, "Dual-frequency ultrasound effect on structure and properties of sweet potato starch," *Starch-Stärke*, vol. 65, no. 7-8, pp. 621–627, 2013.
- [17] M. Tabei, T. D. Mast, and R. C. Waag, "A k-space method for coupled first-order acoustic propagation equations," *The Journal of the Acoustical Society of America*, vol. 111, no. 1, pp. 53–63, 2002.
- [18] T. D. Mast, L. P. Souriau, D.-L. Liu, M. Tabei, A. I. Nachman, and R. C. Waag, "A k-space method for large-scale models of wave propagation in tissue," *IEEE transactions on ultrasonics, ferroelectrics, and frequency control*, vol. 48, no. 2, pp. 341–354, 2001.
- [19] G. Clement, P. White, and K. Hynynen, "Enhanced ultrasound transmission through the human skull using shear mode conversion," *The Journal of the Acoustical Society of America*, vol. 115, no. 3, pp. 1356–1364, 2004.
- [20] G. Van Venrooij, R. Boone, and J. D. van der Gon, "Two-dimensional echo-encephalography," *Acta neurochirurgica*, vol. 49, no. 1, pp. 1–8, 1979.
- [21] J. Bamber, *Acoustical Characterisation of Biological Media Encyclopedia of Acoustics*. New York: Wiley, 1997.
- [22] R. Draï, F. Sellidj, M. Khelil, and A. Benchaala, "Elaboration of some signal processing algorithms in ultrasonic techniques: application to materials ndt," *Ultrasonics*, vol. 38, no. 1-8, pp. 503–507, 2000.
- [23] B. E. Treeby and B. T. Cox, "k-wave: Matlab toolbox for the simulation and reconstruction of photoacoustic wave fields," *Journal of biomedical optics*, vol. 15, no. 2, p. 021314, 2010.